10186 *Inorg. Chem.* **2009**, *48*, 10186–10192
DOI: 10.1021/ic9011668

Inorganic Chemistry
Article

Solid-State NMR Study of Dehydration of Layered α-Niobium Phosphate

Jianfeng Zhu and Yining Huang*

Department of Chemistry, The University of Western Ontario, London, Ontario, Canada N6A 5B7

Received June 17, 2009

The dehydration of a representative layered α-niobium phosphate (α-NbP) was studied by ^{93}Nb solid state wide-line NMR in combination with several other techniques including X-ray diffraction, thermogravimetric analysis, and ^{31}P MAS NMR. Four niobium phosphate species associated with dehydration including tri-, di-, and monohydrate phases, as well as a completely dehydrated phase, are identified by ^{93}Nb NMR. The tri- and dihydrate phases coexist in the as-made α-NbP sample. The monohydrate phase formed after heating the sample at 70 °C, and an additional anhydrous phase was produced when further dehydrated at 140 °C. The dehydration at 250 °C resulted in a completely anhydrous phase. The ^{93}Nb NMR parameters extracted from the wide-line NMR spectra acquired at different magnetic fields are highly sensitive to the dehydration process.

Introduction

Layered metal phosphates, MPs (M = Zr, Ti, Mo, Nb, V, Mg, Hf) are important materials with several applications in ion-exchange, intercalation, catalysis, sorption, protonic conductors, solar energy storage, and crystal engineering.[1−3] α-$NbOPO_4 \cdot 3H_2O$ (α-NbP)[4,5] is the most well-known example of niobium phosphates (NbPs). The structure of α-NbP, although not determined, is widely accepted to be isostructural with α-$VOPO_4 \cdot 2H_2O$ (α-VP).[4] Figure 1 illustrates the structure of the α-NbP proposed based on that of α-VP.[6,7] Each layer contains NbO_6 octahedra, and each NbO_6 octahedron is connected to four PO_4 tetrahedra in the equatorial plane. One of the axial groups in the octahedron is an Nb═O double bond, and the other axial ligand is a water molecule directly bonded to the metal center. The layers are electrically neutral and held together by hydrogen bonding involving the Nb═O group, the coordinated water molecule, as well as the water molecules occluded in the interlayer space. Since the interactions holding the layers together are weak, guest species readily intercalate into the interlayer galleries. The intercalations of organic compounds such as amines[8,9] and alcohols[10,11] into α-NbP have been studied previously using thermogravimetric analysis (TGA) and vibrational spectroscopy.

The layered structure and its intercalation properties make niobium phosphates good candidates for catalysts.[12−14] For example, it has been shown that NbPs are able to promote several acid-catalyzed reactions.[15] In recent years, a family of mixed VP-NbP catalysts have been prepared to selectively oxidize *n*-butane or *n*-butene to maleic anhydride.[16,17] To better understand the applications and to design new NbP-based materials, detailed structure information on these layered materials is needed. However, as is the case for most MPs, it is usually difficult to obtain suitable NbP crystals for single-crystal X-ray diffraction (XRD) studies. Solving the structure by powder XRD is also not straightforward because there are often few diffraction lines for analysis. As a result, only the structure of the anhydrous α-NbP[18] has been determined. It is intriguing to note that the dehydrated phase has a three-dimensional framework rather than the layered structure of the parent material. Therefore, the dehydration process has been an interesting topic and studied by powder XRD,[4,8] infrared (IR) and ^{1}H NMR.[19] In general, it is the

*To whom correspondence should be addressed. E-mail: yhuang@uwo.ca. Phone: 519-661-2111, ext 86384. Fax: 519-661-3022.

(1) Clearfield, A. Costantino, U. *Comp. Supramol. Chem.* **1996**, *V7*, 107, and references therein.
(2) Auerbach, S. M.; Carrado, K. A.; Dutta, R. K. *Handbook of Layered Materials*; Marcel Dekker: New York, 2004; pp 313−371, and references therein.
(3) Forium on Vanadyl Pyrophosphate. Centi, G., Ed.; *Catal. Today* **1994**, *16*, 1−153.
(4) Chernorukov, N. G.; Egorov, N. P.; et al. *Russ. J. Inorg. Chem* **1978**, *23*, 1627.
(5) Hahn, R. B. *J. Am. Chem. Soc.* **1951**, *73*, 5091.
(6) Tietze, H. R. *Aust. J. Chem.* **1981**, *34*, 2035.
(7) Hewat, A. W.; Tachez, M.; Bernard, J. *Rev. Chim. Miner.* **1982**, *19*, 291.
(8) Beneke, K.; Lagaly, G. *Inorg. Chem.* **1983**, *22*, 1503.
(9) Kinomura, N.; Kumada, N. *Inorg. Chem.* **1990**, *29*, 5217.
(10) Benes, L.; Zima, V; Melanova, K. *J. Inclusion Phenom. Macrocyclic Chem.* **2001**, *40*, 131.
(11) Benes, L.; Melanova, K.; Votinsky, J. *J. Solid State Chem.* **1998**, *141*, 64.
(12) Nowak, I.; Ziolek, M. *Chem. Rev.* **1999**, *99*, 3603.
(13) Ziolek, M. *Catal. Today* **2003**, *78*, 47.
(14) Clearfield, A.; Costantino, U. *Comp. Supra. Chem.* **1996**, *V7*, 107.
(15) Okazaki, S.; Wada, N. *Catal. Today* **1993**, *16*, 349.
(16) Duarte de Farias, A. M.; Volta, J.-C. *J. Catal.* **2002**, *208*, 238.
(17) Pries de Oliveira, P. G.; Volta, J. C. *Catal. Today* **2000**, *57*, 177.
(18) Kalousova, J.; Votinsky, J.; Benes, L.; Melanova, K.; Zima, V. *Collect. Czech. Chem. Commun.* **1998**, *63*, 1.
(19) Bruque, S.; Martinez-Lara, M.; Moreno-Real, L.; Jimenez-Lopez, A.; Casal, B.; Ruiz-Hitzky, E.; Sanz, J. *Inorg. Chem.* **1987**, *26*, 847.

Published on Web 09/25/2009

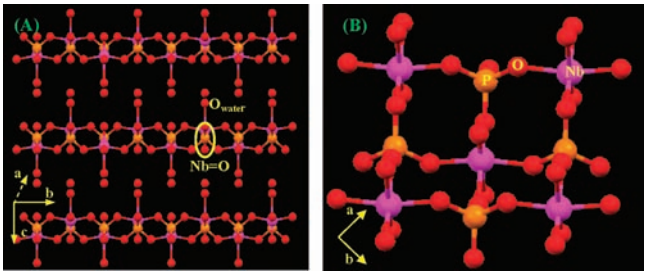

Figure 1. Structure of α-$NbOPO_4 \cdot 3H_2O$ showing (A) the layered structure; (B) the detailed coordination within a layer. The hydrogens are omitted for clarity.

dehydrated phases that are involved in catalysis while the hydrated materials are usually the precursors.

Solid-state NMR is a complementary technique to XRD. However, only one ^{1}H NMR study[19] has been performed for characterization of NbPs. ^{93}Nb solid-state NMR has never been used to directly probe the local environments around Nb in these materials. ^{93}Nb is a quadrupolar nucleus with a spin $I = 9/2$. It has a relative high gyromagnetic ratio comparable to ^{13}C and a high natural abundance (100%). But it also has a relatively large nuclear quadrupole moment ($Q = -3.2 \times 10^{-29}$ m^2),[20] which interacts with any electric field gradients (EFG) at the nucleus, leading to the broad ^{93}Nb spectral lines. In recent years, ^{93}Nb solid-state NMR is increasingly becoming a powerful tool for materials characterization[21,22] and has been used to study different systems including various niobates,[21−25] ferroelectrics,[22,26,27] niobium silicates,[22] niobium phosphates,[28,29] niobium oxyfluorides,[30,31] and half-sandwich niobium cyclopentadienyl complexes.[32]

In the present study, the local environments of the niobium centers in α-NbP and its dehydrated phases were investigated by wide-line ^{93}Nb NMR. The chemical shift (CS) and the electric field gradient (EFG) tensor parameters including the isotropic CS (δ_{iso}), the span (Ω), skew (κ), quadrupolar coupling constant (C_Q), and the EFG tensor asymmetry parameter (η_Q) were extracted by analyzing the ^{93}Nb static spectra. To obtain reliable NMR parameters, the ^{93}Nb spectra were acquired at three different fields, 9.4, 14.1, and 21.1 T. One of the goals of this study is to explore the sensitivity of ^{93}Nb static spectra to the dehydration. ^{31}P magic angle spinning (MAS) NMR, powder XRD, and TGA have also been applied to investigate the dehydration.

Experimental Section

The α-NbP was synthesized by the following procedure:[8,19] 6 g of Nb_2O_5 was refluxed in 42 mL of HF (40%) for 2 days in a Teflon container; 24.6 mL of H_3PO_4 was added to this solution, and the mixture was heated in a steam bath until a crystalline precipitate formed and the solids were then recovered by centrifugation. The precipitate was washed with 5 M HNO_3, then water, and dried at room temperature. This sample is hereafter referred to as the as-made α-NbP. The dehydrated samples were obtained by heating as-made α-NbP in an oven at 70 °C for 2 h, 140 °C for 2 h, and 250 °C for 20 h. The dehydrated samples were kept in sealed tubes for NMR and TGA analysis.

The identity of the synthesized materials was confirmed by comparing the powder XRD patterns with those reported in the literature.[8−11] Powder XRD measurements were performed on a Rigaku Rotating Anode diffractometer (45 kV/160 mA) using graphite-monochromated Co Kα radiation with a wavelength of 1.7902 Å. The powder XRD patterns were recorded within the range $5° \le 2\theta \le 65°$ with 10°/min step width and 6 min count time. The dehydration of α-NbP was also followed by TGA, which was performed on a Mettler Toledo TGA/SDTA851 analyzer. TGA measurements were carried out in a temperature range of 25−550 °C at a heating rate of 10 °C/min. The flow rate of nitrogen gas was 25 mL/min.

^{93}Nb static NMR experiments were performed at three different fields: 9.4 (97.73 MHz), 14.1 T (147.67 MHz), and 21.1 T (220.23 MHz). The experiments at 9.4 T were performed on a Varian Infinityplus 400 WB spectrometer, using a horizontal 5 mm static probe. The static spectra were acquired by using the spin−echo sequence with the phase cycling developed by Oldfield et al.[33] and a 90° refocusing pulse [$\pi/2 - \tau - \pi/2 - \tau$ - acq]. A non-selective $\pi/2$ pulse width of 4.5 μs, corresponding to a selective $\pi/2$ pulse width of 0.9 μs for ^{93}Nb central transition, was calibrated on a 0.4 M $NbCl_5$/CH_3CN solution. A recycle delay of 2.0 s was applied. The ^{93}Nb static spectra at 14.1 T were acquired on a Varian Inova 600 spectrometer, using a 3.2-mm MAS probe. The experiments at 21.1 T were performed on a 900 MHz Bruker Avance II spectrometer at the *National Ultrahigh-field NMR Facility for Solids* in Ottawa, Canada, using a 4 mm MAS probe. ^{93}Nb CSs were referenced to a 0.4 M $NbCl_5$/CH_3CN solution ($\delta_{iso} = 0$ ppm).

The ^{31}P NMR experiments were performed on the same Varian Infinityplus 400 WB spectrometer. A 5 mm MAS probe was used, and the samples were spun at 10 kHz. A $\pi/6$ pulse (1.5 μs) and a recycle delay of 60 s were applied.

All spectral simulations were carried out by using the WSOLIDS1 software package.[34] The experimental error for each measured parameter was determined by visual comparison of experimental spectra with simulations. The parameter of concern was varied bidirectionally starting from the best fit value, and all other parameters were kept constant, until noticeable differences between the spectra were observed.

The calculations of the CS and EFG tensors of ^{93}Nb in the dehydrated NbP phases were performed using the Gaussian

(20) Pyykko, P. *Mol. Phys.* **2001**, *99*, 1617.
(21) MacKenzie, K. J. D.; Smith, M. E. *Multinuclear Solid State NMR of Inorganic Materials*; Pergamon: Oxford, 2002.
(22) Lapina, O. B.; Khabibulin, D. F.; Shubin, A. A.; Terskikh, V. V. *Prog. Nucl. Magn. Reson. Spectrosc.* **2008**, *53*, 128, and references therein.
(23) Lapina, O. B.; Khabibulin, D. F.; Romanenko, K. V.; Gan, Z.; Zuev, M. G.; Krasil'nikov, V. N.; Fedorov, V. E. *Solid State Nucl. Magn. Reson.* **2005**, *28*, 204.
(24) Wang, X.; Smith, L. J. *J. Mol. Catal. A* **2008**, *281*, 214.
(25) Modeshia, D. R.; Darton, R. J.; Ashbrook, S. E.; Walton, R. I. *Chem. Commun.* **2009**, 68.
(26) Vold, R. L.; Hoatson, G. L.; Vijayakumar, M. *Phys. Rev. B* **2007**, *75*, 134105/1.
(27) Hoatson, G. L.; Zhou, D. H.; Fayon, F.; Massiot, D.; Vold, R. L. *Phys. Rev. B* **2002**, *66*, 224103.
(28) Flambard, A.; Montagne, L.; Delevoye, L.; Palavit, G.; Amoureux, J.-P.; Videau, J.-J. *J. Non-Cryst. Solids* **2004**, *345−346*, 75.
(29) Flambard, A.; Montagne, L.; Delevoye, L.; Steuernagel, S. *Solid State Nucl. Magn. Reson.* **2007**, *32*, 34.
(30) Du, L.-S.; Schurko, R. W.; Lim, K. H.; Grey, C. P. *J. Phys. Chem. A* **2001**, *105*, 760.
(31) Du, L.-S.; Schurko, R. W.; Lim, K. H.; Grey, C. P. *J. Phys. Chem. A* **2002**, *106*, 7876.
(32) Lo, A. Y. H.; Bitterwolf, T. E.; Macdonald, C. L. B.; Schurko, R. W. *J. Phys. Chem. A* **2005**, *109*, 7073.
(33) Kunwar, A. C.; Turner, G. L.; Oldfield, E. *J. Magn. Reson.* **1986**, *69*, 124.
(34) Eichele, K.; Wasylishen, R. E. *WSOLIDS1 NMR Simulation Package*, 1.17.30; 2001.

03 program[35] on SHARCNET (www.sharcnet.ca).[36] The calculations were carried out with simplified molecular clusters containing the structural units of interest, specifically $Nb(PO_4)_4(NbO_6)_2H_{18}^{3-}$ (**1**) for the dehydrate phase and $Nb(PO_4)_4O(H_2O)H_8^-$ (**2**) for the monohydrate phase. Cluster **1** was truncated from the periodic lattice of anhydrous α-NbP[18] and terminated with OH groups, an approach widely used in ab initio calculations of ^{27}Al EFG tensors in periodic solids such as zeolites.[37−41] The H atoms used to terminate the cluster were placed in the fourth coordination sphere of the central Nb atom replacing either the P or the Nb atoms connected to the O atoms. No further optimization was performed. Cluster **2** was constructed by replacing the two axial NbO_6 units in cluster **1** with O and H_2O group. The NMR parameters were then calculated by systematically varying the Nb═O and Nb−OH_2 bond distances. The calculations were carried out using the restricted Hartree−Fock (RHF) method. Two expanded all-electron basis sets,[42] 4F(43333/433/43) and 6D(43333/433/43) corresponding to valence shell electron configurations of $4d^35s^2$ and $4d^45s^1$, respectively, were applied for Nb. Basis set of 6-311G** was applied to all the atoms other than Nb.

The calculated EFGs (V_{XX}, V_{YY}, V_{ZZ}) were converted to the quadrupole coupling constant (C_Q) and asymmetry parameter (η_Q) according to the following definition: $|V_{XX}| \leq |V_{YY}| \leq |V_{ZZ}|$; $C_Q = (eV_{ZZ}Q/h) \times 9.71736 \times 10^{21}$ (Hz); $\eta_Q = (V_{XX} - V_{YY})/V_{ZZ}$, where e is the electric charge; Q is the nuclear quadrupole moment [$Q(^{93}Nb) = -3.2 \times 10^{-29}$ m^2];[20] h is Planck's constant. The constant of 9.71736×10^{21} in the equation is due to V_{ZZ} being calculated in atomic units (1 au = 9.71736×10^{21} V·m^{-2}). For Gaussian calculations, the above conversion can be obtained automatically by using the EFGShield program.[43] The calculated chemical shielding, σ, was converted to CS using $NbCl_6^-$ (δ_{iso} = 0.0 ppm) as the primary reference,[32] according to the equation: δ (ppm) = σ_{ref} (ppm) − σ_{sample} (ppm). The absolute shielding of the reference compound was obtained from a geometry-optimized $NbCl_6^-$ ion, using the same method and basis set as for the clusters. The three principal components of the CS tensor are defined as $|\delta_{11}| \geq |\delta_{22}| \geq |\delta_{33}|$. The span Ω and skew κ are defined as follows: $\Omega = \delta_{11} - \delta_{33}$ and $\kappa = 3(\delta_{22} - \delta_{iso})/\Omega$.

Results and Discussion

The as-made α-NbP was dehydrated at different temperatures under the literature conditions,[19] and the resulting powder XRD patterns are consistent with those reported in the literature (Supporting Information, Figure S1A-D). The parent, as-made α-NbP has an interlayer distance of 8.1 Å obtained from the XRD pattern, which is in good agreement with the literature value.[4] After dehydration at 70 °C for 2 h, a new layered structure with an interlayer distance of 6.9 Å was formed. When as-made α-NbP was heated at 140 °C for 2 h, a layered structure with an interlayer spacing of 6.1 Å was obtained. After heating at 250 °C for 20 h, anhydrous NbP was produced as indicated by the XRD pattern.

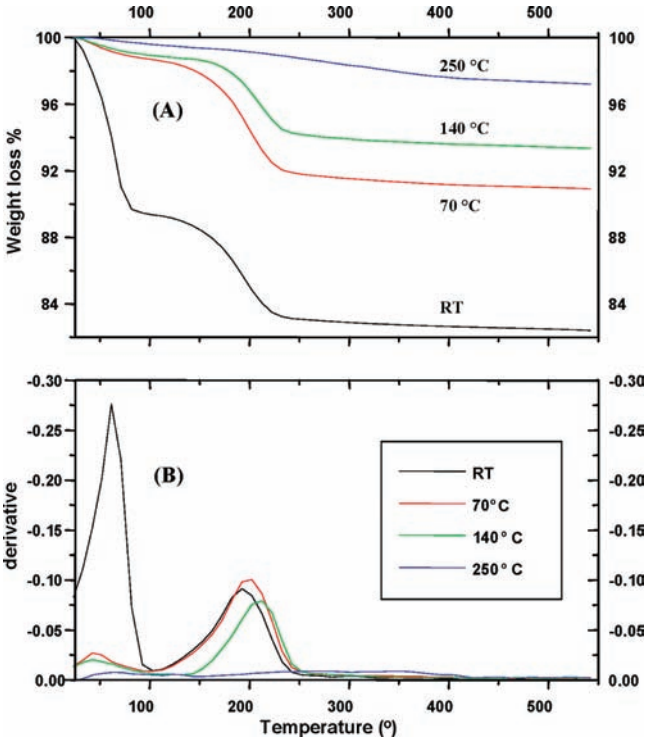

Figure 2. (A) TGA and (B) DTA curves of as-made α-NbP samples dehydrated at different temperatures.

To obtain further information about the dehydrated phases, TGA experiments were performed (Figure 2A). The TGA curve of as-made α-NbP shows two steps of weight loss, indicating the existence of two different types of water molecules. Taking the derivative of the TGA curve yields the corresponding differential thermal analysis (DTA) curve (Figure 2B). The DTA curve of as-made α-NbP shows two peaks at around 70 and 200 °C. The peak at around 70 °C is due to the loss of the water molecules occluded between the layers, and the peak at 200 °C originates from the removal of the water molecules directly coordinated to the Nb. The weight loss in the TGA suggests that there are about 1.3 interlayer water molecules and one coordinated water molecule; therefore, instead of 3, a total of 2.3 water molecules per formula exist in the structure. The results indicate that the as-made α-NbP is a mixture of trihydrate (30%) and dihydrate (70%) phases. However, the XRD pattern (Supporting Information, Figure S1A) is identical to those reported for α-$NbOPO_4 \cdot 3H_2O$, suggesting that partially losing one water molecule to become the dihydrate phase does not change the layered structure significantly. This is probably due to the high mobility of the interlayer water molecules. A similar situation was observed in a previous ^{1}H and IR study.[19]

The TGA and DTA curves of the sample dehydrated at 70 °C for 2 h show mainly one peak at about 200 °C corresponding to the weight loss of the water molecules directly bonded to the Nb centers. This suggests that the 70 °C sample is a pure monohydrate phase. The TGA and DTA curves of the 140 °C sample are very similar to those of the 70 °C sample. The weight loss corresponds to the removal of 0.69 water molecules per formula, suggesting this sample is a mixture of monohydrate phase (69%) and anhydrous phase

(35) Frisch, M. J.; Trucks, G. W.; Schlegel, H. B.; Scuseria, G. E. et al. *Gaussian 03*, Revision C.02; Gaussian, Inc.: Wallingford, CT, 2004.
(36) Shared Hierarchial Academic Research Computing Network; www.sharcnet.ca.
(37) Simperler, A.; Anderson, M. W.; et al. *J. Phys. Chem. B* **2002**, *106*, 10944.
(38) García-Serrano, L. A.; Zaragoza, I. P.; et al. *J. Mol. Catal. A* **2003**, *200*, 205.
(39) Tielens, F.; Geerlings, P.; et al. *J. Phys. Chem. B* **2003**, *107*, 11065.
(40) Bucko, T.; Hafner, J.; Benco, L. *J. Chem. Phys.* **2004**, *120*, 10263.
(41) Soscun, H.; Castellano, O.; Hernandez, J. *J. Phys. Chem. B* **2004**, *108*, 5620.
(42) *Gaussian Basis sets for Molecular Calculations*; Huzinaga, S., Ed.; Elsevier: New York, 1984.
(43) Adiga, S.; Aebi, D.; Bryce, D. L. *Can. J. Chem.* **2007**, *85*, 496.

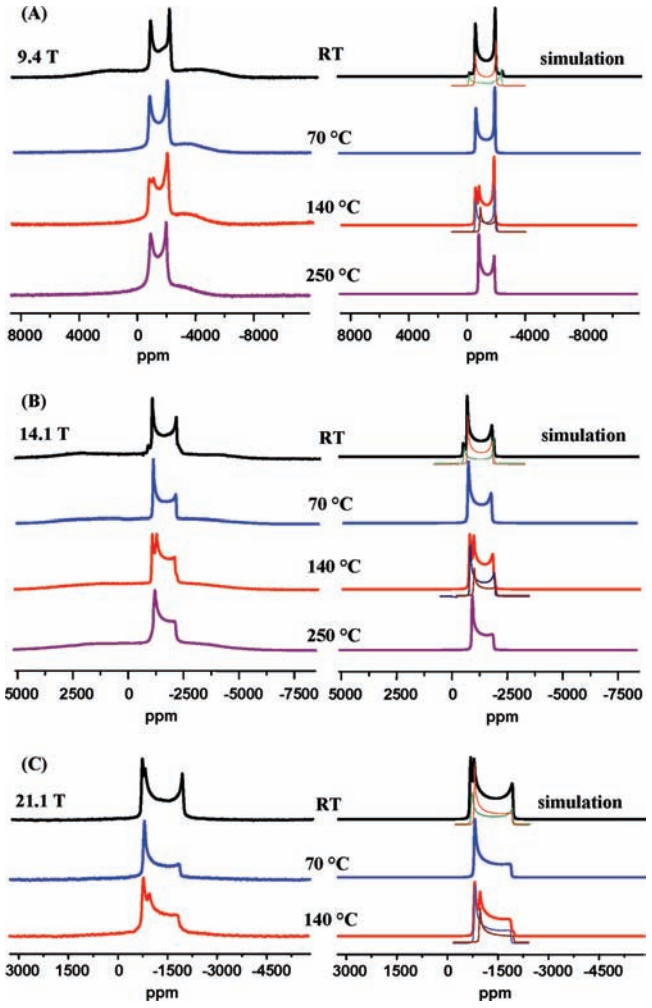

Figure 3. ^{93}Nb static NMR spectra of as-made α-NbP and its dehydrated phases at the magnetic fields of (A) 9.4, (B) 14.1, and (C) 21.1 T. The very broad signals near the baseline in the spectra are due to a small amount of unreacted Nb_2O_5.

(31%). It is noted that although the samples dehydrated at 70 and 140 °C both have the monohydrate phases, their interlayer distances are slightly different (6.9 Å for the 70 °C sample and 6.1 Å for the 140 °C sample). These phenomena were also reported by other groups.[8,19] It appears that the interlayer spacing of the monohydrate phase depends on the thermal history. The sample dehydrated at 250 °C is the anhydrous phase. A very small amount of weight loss (less than 2%) in the TGA curve is due to the residual monohydrate phase as shown by ^{31}P MAS NMR spectrum (see discussion later).

The ^{93}Nb static NMR spectra of as-made α-NbP and its dehydrated phases (Figure 3) were obtained to probe the effect of dehydration on the environment of the Nb centers. Since there is only one crystallographic Nb site in α-NbP, there should be only one ^{93}Nb resonance in the spectrum. However, the ^{93}Nb NMR spectra at 14.1 and 21.1 T both clearly exhibit two signals. This confirms the TGA results that the as-made NbP sample is a mixture of tri- and dihydrate phases. Indeed, the spectra at 3 different fields can be well fitted by two Nb sites, and their NMR parameters were given in Table 1. A comparison of the NMR intensity with the TGA weight loss ratio of the tri- and dihydrate phases allows one to assign the ^{93}Nb resonance with an isotropic shift, δ_{iso}, at −1160 ppm to the trihydrate phase and the single with a $\delta_{iso} = -1130$ ppm to the dihydrate phase. The signals became broader with increasing field strengths from ~150 (at 9.4 T) to 190 (at 14.1 T) to 260 kHz (at 21.1 T), indicating that the spectra are dominated by the CS anisotropy (CSA). The values of skew κ are 0.93 and 1.0 for di- and trihydrate phases, respectively, which indicates approximately axial CS tensors for both materials. Indeed, the large CSA values were obtained from spectral simulations (Table 1), confirming the dominance of the CSA. The C_Q values of tri- and dihydrate phases are 45 and 30 MHz, respectively. Similar C_Q values have been reported for different niobates[22,23] and niobium phosphates.[28,29] The value of η_Q for both tri- and dihydrate phases are equal to zero, implying that the V_{ZZ} component is the unique component of the EFG tensor. The Euler angles of (0, 0, 0) suggest that the two axis systems describing the CS and the EFG tensors coincide with each other. These results imply that there is an approximate local C_4 axis along the axial O=Nb−OH_2 direction. The very broad weak signal near baseline is due to the unreacted Nb_2O_5.

The ^{93}Nb static NMR spectra of the sample dehydrated at 70 °C (Figure 3) were also acquired at three different magnetic fields. They exhibit only one signal, consistent with the TGA result that this sample is a pure phase of monohydrate NbP. Again, the broader resonance at higher field suggests predominate contribution from the CSA. Simulating the spectra yields the following CS and EFG parameters: $\delta_{iso} = -1180$ ppm, $\Omega = 1068$ ppm, $\kappa = 0.93$, $C_Q = 28$ MHz, $\eta_Q = 0.00$. Figure 4 illustrates the simulated spectra emphasizing the individual contributions from the CS and the quadrupolar interactions at different fields, and they clearly demonstrate the dominance of the CSA in the spectra, especially at 21.1 T. It is also noted that a large C_Q value of 28 MHz only produces a relatively narrow signal less than 100 kHz. This is because for a half-integer spin nucleus at static condition the second-order quadrupolar broadening of the central transition is proportional to υ_Q^2/υ_0, where υ_Q is the quadrupolar frequency, $3C_Q/[2I(2I-1)]$, and υ_0 is the Larmor frequency.[21,44] Therefore, the broadening corresponding to a given C_Q value decreases as the spin quantum number I increases.

The ^{93}Nb static NMR spectra of the sample dehydrated at 140 °C show two signals (Figure 3): one is the same as that of the 70 °C sample and the other one is slightly narrower but with a similar line-shape. The former can be assigned to the Nb in the monohydrate phase; the latter must be due to the Nb in the anhydrous material. For each Nb site, the spectra at three fields can be well simulated by using a single set of CS and EFG parameters which are listed in Table 1. The ^{93}Nb static NMR spectra of the sample dehydrated at 250 °C were also acquired (Figure 3). The spectra taken at different fields can be well simulated with a single ^{93}Nb resonance, which agrees well with the crystal structure determined by single crystal X-ray diffraction[18] showing that the completely dehydrated α-NbP has only a single Nb site. The value of $\kappa = 0.93$ is very close to 1, suggesting a CS tensor with an approximate axial symmetry. The value of asymmetry parameter ($\eta_Q = 0.0$) indicates an axial EFG tensor. The X-ray structure shows that the Nb atom is slightly above the plane

(44) Duer, M. J. *Solid-State NMR Spectroscopy: Principles and Applications*; Blackwell Science: Oxford, 2002.

Table 1. Parameters Used to Fit ^{93}Nb Static Spectra of As-Made α-NbP and Its Dehydrated Phases

compounds		δ_{iso}(ppm)	Ω (ppm)	κ	C_Q(MHz)	η_Q	intensity
RT	site 1	−1130 ± 10	1150 ± 20	0.93 ± 0.05	45 ± 2	0.00 ± 0.02	23%
	site 2	−1160 ± 10	1100 ± 20	1.00 ± 0.05	30 ± 2	0.00 ± 0.02	77%
70 °C		−1180 ± 10	1068 ± 20	0.93 ± 0.05	28 ± 2	0.00 ± 0.02	
140 °C	site 1	−1180 ± 10	1068 ± 20	0.93 ± 0.05	28 ± 2	0.00 ± 0.02	67%
	site 2	−1300 ± 10	1017 ± 20	0.93 ± 0.05	20 ± 2	0.00 ± 0.02	33%
250 °C		−1300 ± 10	1017 ± 20	0.93 ± 0.05	20 ± 2	0.00 ± 0.02	

[a] For all the simulations, the Euler angles (α, β, γ) are (0, 0, 0).

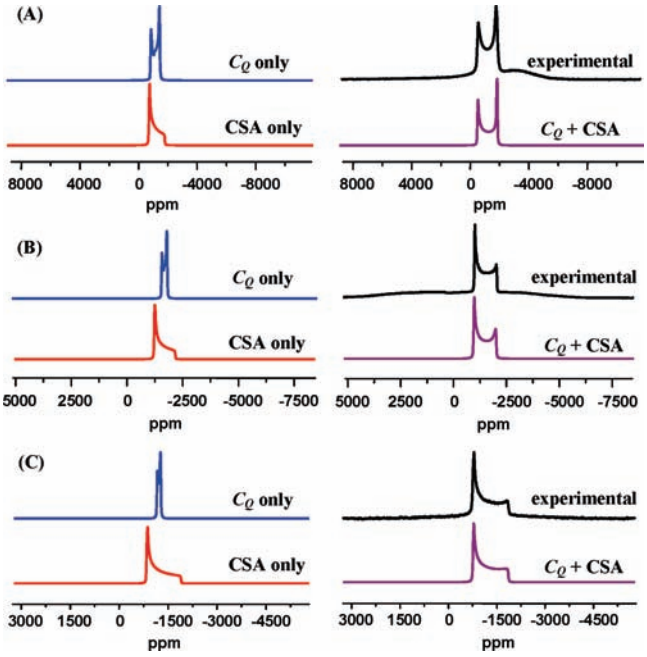

Figure 4. Observed and simulated ^{93}Nb static spectra of the sample dehydrated at 70 °C at the magnetic fields of (A) 9.4, (B) 14.1, and (C) 21.1 T, showing the contributions of the CSA and the EFG to the observed spectra.

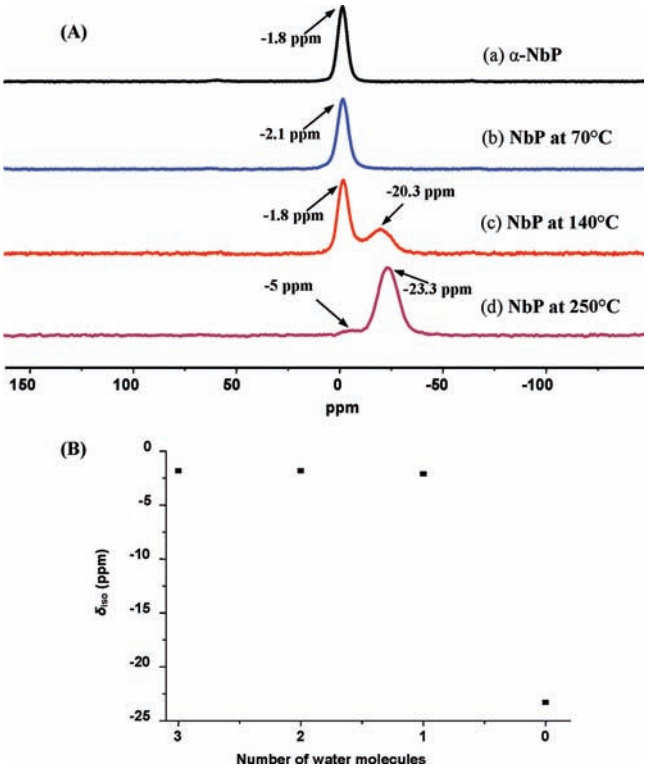

Figure 5. (A) ^{31}P MAS spectra of as-made α-NbP and its dehydrated phases. (B) The relationship between the number of water molecules in the lattice of α-NbP and ^{31}P isotropic CS.

defined by 4 equatorial oxygen atoms. Although the true crystallographic site symmetry of Nb is merely C_2, the facts that 4 Nb−O bonds perpendicular to the C_2 have identical bond distances and that the distortion of the NbO_6 octahedron is mainly along the crystallographic C_2 render an approximate local C_4 collinear with the true C_2, which explains the observed tensor symmetry. The CS and EFG parameters extracted from spectral simulation are identical to the second signal seen in the spectra of the 140 °C sample discussed earlier, confirming the existence of anhydrous phase in the sample dehydrated at 140 °C.

The ^{93}Nb CS values of all four phases fall in the region of NbO_6 octahedra reported in the literature.[22] An inspection of Table 1 reveals that the dehydration induces a downfield CS, a decrease in the CSA, and a reduction of C_Q. These results indicate that the dehydration leads to a more symmetric Nb local environment in NbO_6 octahedra because (1) the water molecules are gradually removed from the lattice and (2) the Nb=O double bond is gradually lengthened and eventually transforms to a Nb−O single bond. Supporting Information, Figures S2A−C show approximate linear relationships between the ^{93}Nb NMR parameters (including δ_{iso}, Ω, and C_Q) and the number of water molecules in the lattice. These correlations indicate that the ^{93}Nb NMR parameters are sensitive to the dehydration.

^{31}P MAS spectra, on the other hand, appear not very sensitive to the number of the water molecule in the lattice. Figure 5A shows that the as-made α-NbP only has a single broad ^{31}P peak at −1.8 ppm. This suggests only one P environment, which is different from the ^{93}Nb NMR result. The sample dehydrated at 70 °C shows essentially the same ^{31}P signal. It appears that the tri-, di-, and monohydrate phase all exhibit the same ^{31}P peak. The sample dehydrated at 140 °C exhibits two ^{31}P signals: one is the same as that observed in the 70 °C sample and the other one at −20.3 ppm is similar to that seen in the 250 °C sample, confirming that the 140 °C sample is a mixture of the monohydrate phase and the anhydrous phase. In addition to the signal at −23.3 ppm originating from P in the anhydrous phase, the ^{31}P MAS spectrum of the 250 °C sample also has a very small signal, indicating the existence of a very small amount of residual monohydrate phase present in the 250 °C sample, which is consistent with the TGA results. The results show that overall the ^{31}P isotropic CSs are less sensitive to the dehydration until the anhydrous phase is formed (Figure 5B). The possible reason is that the occluded interlayer water molecules are hydrogen bonded to the oxygen atom in Nb=O group as well

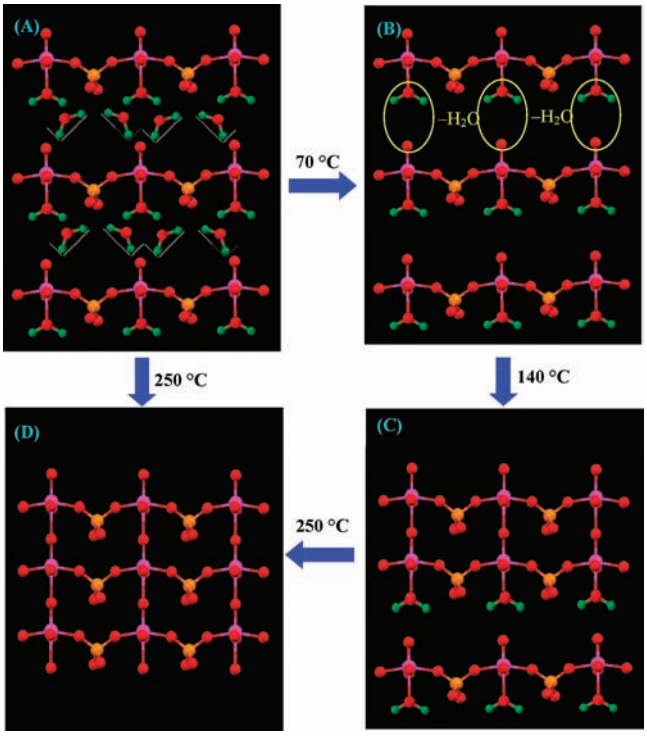

Figure 6. Schematic illustration of the dehydration process.

as the water molecule directly coordinated to Nb, but not to the oxygen atoms bridging the Nb and the PO_4 groups (Figure 6A). Consequently, the departure of the occluded water molecules from the lattice affects the Nb local structure more than the P environment. It is interesting to notice that the η_Q and skew κ remain essentially unchanged during the dehydration process (Table 1 and Supporting Information, Figure S2D), suggesting that during the dehydration the C_4 local symmetry is preserved.

To confirm this argument, theoretical calculations of the NMR tensor properties were carried out since a recent study showed that the ^{93}Nb CS and EFG tensor parameters, especially the latter, can be predicted reasonably well with the RHF method.[32] Therefore, we performed RHF calculations on two model clusters representing the monohydrate and completely dehydrate phases. For dehydrate phase, a cluster of $Nb(PO_4)_4(NbO_6)_2H_{18}^{3-}$ (**1**) was truncated from its periodic lattice (Figure 7A). The cluster adopts the same geometry of the anhydrous α-NbP, and no further optimization was performed. Our previous work on layered ZrP[45] and TiP[46] has shown that the clusters with similar sizes are adequate for the calculations of metal center NMR parameters in layered metal phosphates. The ^{93}Nb CS and EFG tensor parameters were calculated by using two basis sets: 4F(43333/433/43) and 6D(43333/433/43) and the results are give in Table 2. The calculations using both basis sets predict a symmetric CS ($\kappa \approx 1$) and EFG tensor ($\eta_Q \approx 0$), confirming the existence of an approximate 4-fold axis. The calculations show that the directions of V_{zz} (the largest EFG tensor component) and δ_{33} (the most shielded CS tensor component) are indeed along the axial direction (Figure 7).

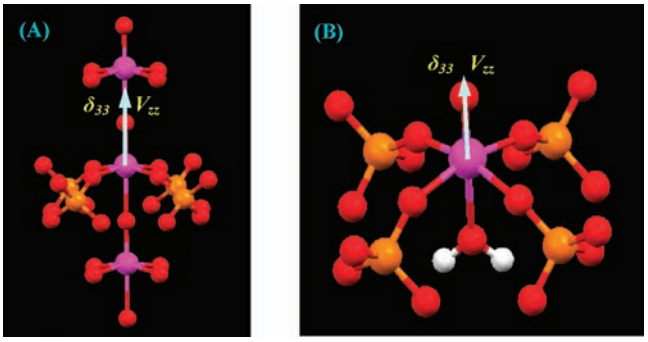

Figure 7. Structures of the model clusters (A) $Nb(PO_4)_4(NbO_6)_2H_{18}^{3-}$ and (B) $Nb(PO_4)_4O(H_2O)H_8^{-}$ representing completely anhydrous and mono-hydrate α-NbP, respectively. The directions of V_{zz} and δ_{33} obtained via RHF calculations using a 4F(43333/433/43) basis set for Nb are indicated on the clusters. The H atoms are omitted for clarity except those of the water molecule directly bonded to the Nb.

Table 2. Calculated NMR Parameters of the Cluster $Nb(PO_4)_4(NbO_6)_2H_{18}^{3-}$ Representing Anhydrous Phase

samples	basis sets	δ_{iso} (ppm)	Ω (ppm)	κ	C_Q (MHz)	η_Q
anhydrous	4F	−1354	2315	1.00	20.3	0.00
	6D	−1201	2160	1.00	30.4	0.00
	expt.	−1300	1017	0.93	20	0.00

4F(43333/433/43) basis set yields a C_Q value close to the experimental value, but 6D(43333/433/43) basis set overestimates the quadrupolar coupling constant. The CSA are not well predicted due probably to that the relativistic effect,[47] which is very important for heavy elements, is not included in the calculations for Nb. The crystal structure of monohydrated phase is not known. We constructed a cluster by taking the coordinates of the Nb and 4 PO_4 within the layer from the anhydrous phase (Figure 7B) and calculated the NMR parameters by varying the distances between niobium and oxygens corresponding to the axial Nb−OH_2 and the Nb=O bonds. The results are summarized in Figure 8 and Supporting Information, Table S1. For a given basis set, the C_Q and Ω values change significantly with changing bond lengths, but the skew and asymmetry parameters remain very close to unity and zero, respectively. This result clearly confirms that the elongation of the two axial Nb−O bonds occurring during dehydration has little effect on the NbO_4 unit and the 4 PO_4 groups in the second coordination sphere. Supporting Information, Table S1 shows that when the Nb=O is in the range of 1.57−1.65 Å and the Nb−OH_2 is 2.4 Å, the calculated C_Q and Ω are closer to the observed values with 4F(43333/433/43) basis set yielding better results. The best C_Q and Ω values were obtained using 4F(43333/433/43) basis set when Nb=O and Nb−O distances are 1.60 Å and 2.4 Å. It is noted that the above-mentioned Nb−O distances are typical of those Nb−O double and single bond lengths.[48−50] The corresponding V=O and V−O distances in α-VP are 1.567 and 2.233 Å.[6,7] The approach of combining theoretical calculation on molecular model and solid-state

(45) Yan, Z.; Kirby, C. W.; Huang, Y. *J. Phys. Chem. C* **2008**, *112*, 8575.
(46) Zhu, J.; Trefiak, N.; Woo, T. K.; Huang, Y. *J. Phys. Chem. C* **2009**, *113*, 10029.
(47) Schreckenbach, G.; Ziegler, T. *Int. J. Quantum Chem* **1997**, *61*, 899.
(48) Zid, M. F.; Jouini, T.; Piffard, Y. *J. Solid State Chem.* **1992**, *99*, 201.
(49) Ulutagay, M.; Schimek, G. L.; Hwu, S.-J.; Taye, H. *Inorg. Chem.* **1998**, *37*, 1507.
(50) McQueen, T.; Xu, Q.; Andersen, E. N.; Zandbergen, H. W.; Cava, R. J. *J. Solid State Chem.* **2007**, *180*, 2864.

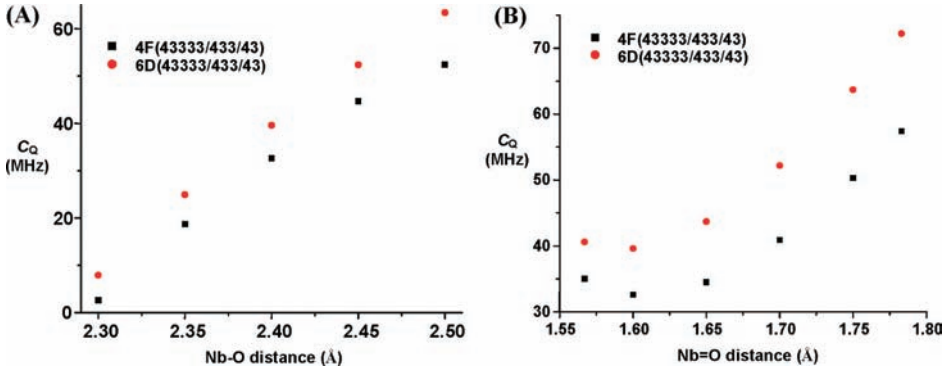

Figure 8. Calculated ^{93}Nb C_Q vs Nb−OH_2 (A) and Nb═O (B) distances. For (A), the Nb═O distance is fixed at 1.6 Å; for (B), the Nb−OH_2 distance is fixed at 2.4 Å.

NMR measurement has been widely applied to understand the local environments around various metal centers in periodic solids containing Mg,[51] Ca,[52] Ti,[46] V,[53,54] Zr,[45,51] Mo,[55] Ag,[56] Bi,[57] and K.[58]

On the basis of the XRD, TGA, and, in particular ^{93}Nb NMR results, the dehydration process of α-NbP can be described as follows (Figure 6). Treating the as-made α-NbP at 70 °C drives the interlayer water molecules off the lattice, leading to the formation of the monohydrate phase. When further heating at 140 °C, the NbP loses its last water molecule directly attached to the Nb center, and at the same time the Nb═O double bond opens up and this oxygen will coordinate to the Nb in the adjacent layer by occupying the coordination site vacated because of the departure of the water molecule. As a result, the layers join together to form the three-dimensional framework of the anhydrous phase. The transformation is complete at 250 °C.

Summary

The dehydration of α-NbP was studied by ^{93}Nb solid-state NMR in combination with other techniques such as XRD and TGA. Four NbP species associated with the dehydration were clearly identified by analyzing ^{93}Nb wide-line spectra acquired at different magnetic fields. The ^{93}Nb CS and EFG parameters are highly sensitive to the number of water molecules in the lattice. The high-resolution ^{31}P MAS spectra, on the other hand, seem to be insensitive to the dehydration. For this series of closely related NbP materials, chemical shielding interaction appears to be dominating the ^{93}Nb spectra.

Acknowledgment. Y.H. acknowledges the financial support from NSERC of Canada for a research grant and CFI for the equipment grants. Funding from the Canada Research Chair program is also gratefully acknowledged. Access to the 900 MHz NMR spectrometer was provided by the *National Ultrahigh Field NMR Facility for Solids* (Ottawa, Canada), a national research facility funded by the Canada Foundation for Innovation, the Ontario Innovation Trust, Recherche Québec, the National Research Council Canada, and Bruker BioSpin and managed by the University of Ottawa (http://www.nmr900.ca). We thank Drs. Terskikh, Pawsey, and Kirby for the technical assistance in NMR experiments, Prof. Wasylishen for the software WSOLIDS1, and Chhatra Khadka for performing the TGA experiments. Computing resources were made available by SHARCnet, Canada Foundation for Innovation, the Ontario Innovation Trust, and IBM of Canada. We thank three anonymous reviewers for their insightful comments and suggestions.

Supporting Information Available: Additional information as noted in the text. This material is available free of charge via the Internet at http://pubs.acs.org.

(51) Zhu, J.; Lin, Z.; Yan, Z.; Huang, Y. *Chem. Phys. Lett.* **2008**, *461*, 260.
(52) Bryce, D. L.; Bultz, E. B.; Aebi, D. *J. Am. Chem. Soc.* **2008**, *130*, 9282.
(53) Gee, B. A. *Solid State Nucl. Magn. Reson.* **2006**, *30*, 171.
(54) Lo, A. Y. H.; Hanna, J. V.; Schurko, R. W. *Appl. Magn. Reson.* **2007**, *32*, 691.
(55) Forgeron, M. A. M.; Wasylishen, R. E. *J. Am. Chem. Soc.* **2006**, *128*, 7817.
(56) Hamaed, H.; Lo, A. Y. H.; May, L. J.; Taylor, J. M.; Shimizu, G. H.; Schurko, R. W. *Inorg. Chem.* **2008**, *47*, 11245.
(57) Hamaed, H.; Laschuk, M. W.; Terskikh, V. V.; Schurko, R. W. *J. Am. Chem. Soc.* **2009**, *131*, 8271.
(58) Moudrakovski, I. L.; Ripmeester, J. A. *J. Phys. Chem. B* **2007**, *111*, 491.